

Lawrence Berkeley National Laboratory

Recent Work

Title

SEMICLASSICAL THEORY OF COLLISIONALLY INDUCED FINE-STRUCTURE TRANSITIONS IN FLUORINE ATOMS

Permalink

<https://escholarship.org/uc/item/5rb7m007>

Authors

Preston, Richard K.

Sloane, Chris

Miller, William H.

Publication Date

1974-02-01

SEMICLASSICAL THEORY OF COLLISIONALLY INDUCED
FINE-STRUCTURE TRANSITIONS IN FLUORINE ATOMS

Richard K. Preston, Chris Sloane and William H. Miller

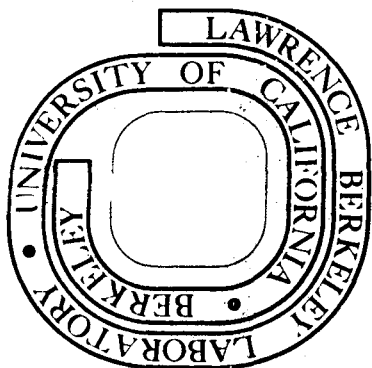
February 1974

Prepared for the U. S. Atomic Energy Commission
under Contract W-7405-ENG-48

RECEIVED
LAWRENCE
RADIATION LABORATORY

MAR 5 1974

LIBRARY AND
DOCUMENTS SECTION



TWO-WEEK LOAN COPY

*This is a Library Circulating Copy
which may be borrowed for two weeks.
For a personal retention copy, call
Tech. Info. Division, Ext. 5545*

LBL-2578
c. 2

DISCLAIMER

This document was prepared as an account of work sponsored by the United States Government. While this document is believed to contain correct information, neither the United States Government nor any agency thereof, nor the Regents of the University of California, nor any of their employees, makes any warranty, express or implied, or assumes any legal responsibility for the accuracy, completeness, or usefulness of any information, apparatus, product, or process disclosed, or represents that its use would not infringe privately owned rights. Reference herein to any specific commercial product, process, or service by its trade name, trademark, manufacturer, or otherwise, does not necessarily constitute or imply its endorsement, recommendation, or favoring by the United States Government or any agency thereof, or the Regents of the University of California. The views and opinions of authors expressed herein do not necessarily state or reflect those of the United States Government or any agency thereof or the Regents of the University of California.

SEMICLASSICAL THEORY OF COLLISIONALLY INDUCED FINE-STRUCTURE
TRANSITIONS IN FLUORINE ATOMS*

Richard K. Preston, Chris Sloane, and William H. Miller[†]

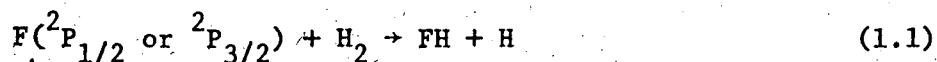
Department of Chemistry, and Inorganic
Materials Research Division, Lawrence
Berkeley Laboratory; University of California,
Berkeley, California 94720

ABSTRACT

A calculation of fine-structure transitions in F atoms impinging on both Xe and H^+ has been carried out using a novel semiclassical theory which was proposed recently by Miller and George. The theory has the advantage of being conceptionally simple and applicable to a wide class of situations. For Xe + F the cross section for the $^2P_{3/2} \rightarrow ^2P_{1/2}$ excitation of F rises from its threshold (0.05 eV) to a value of $\sim 0.1 \text{ \AA}^2$ at a collision energy of 0.5 eV. The cross section for $H^+ + F$ is much larger, reaching a value of $\sim 1 \text{ \AA}^2$ at a collision energy of 0.25 eV, in reasonable agreement with recent quantum mechanical calculations.

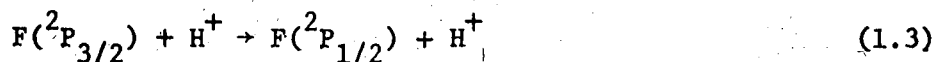
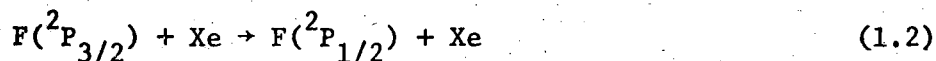
I. INTRODUCTION

Fine-structure transitions can play an important role in inelastic atom-atom collisions at low energy, and there has been considerable theoretical effort expended in the description of this phenomenon.¹⁻³ In the last year, for example, two quantum mechanical studies have appeared which solve the coupled equations numerically with realistic molecular interactions; Mies⁴ investigated transitions in the $F + H^+$ system while Reid⁵ studied the $Na^* + He$ system. It has also been noted^{6,7} that fine-structure transitions can play a significant role in atom-diatom collisions, such as



by determining the fraction of incident atoms that actually enter on the reactive potential energy surface.

This paper reports calculations of cross sections for the low energy processes



utilizing the semiclassical model recently proposed by Miller and George.⁸ Fine-structure transitions present an interesting and challenging test for the semiclassical model, for here there

is no obvious "avoided intersection" of the adiabatic potential curves. Nevertheless, the transition is localized and can be described as taking place at a "complex crossing point" of the adiabatic potentials.⁹

This semiclassical treatment is, of course, not as accurate as a fully quantum mechanical coupled channel calculation which can be readily carried out for these atom-atom systems, but it has the advantage that it can be applied to more general collision systems, such as Eq. (1.1) above, while still incorporating the full classical mechanics of all the heavy particle degrees of freedom. (A fully quantum mechanical coupled channel treatment for an atom-diatom system is unrealistic because of the large number of rotational and vibrational states of the diatom.) To the extent that the semiclassical description of electronic transitions is accurate, therefore, there is the possibility of extending models such as Tully and Preston's trajectory "surface-hopping model"¹⁰ to treat nonadiabatic transitions between potential energy surfaces that have no avoided intersection.

Section II first summarizes the semiclassical theory as it applies to atom-atom collisions, and the potential curves which are used are described in Section III. The results of the calculations are presented and discussed in Section IV and Section V, and Section VI summarizes the results and conclusions.

II. SUMMARY OF SEMICLASSICAL THEORY.

For electronic transitions in low energy atom-atom collisions Miller and George's treatment⁸ reduces essentially to Stueckelberg's model.¹¹ (The principle emphasis of their work⁸ was to extend this, within a dynamically exact description of heavy particle dynamics, to more general, for example atom-diatom, collision systems.) Thus if $V_1(r)$ and $V_2(r)$ are the adiabatic potential curves for electronic states 1 and 2, the $1 \rightarrow 2$ electronic transition takes place along the classical trajectory which changes potential curves at the complex crossing point r_* , i.e., the root of

$$\Delta V(r) \equiv V_2(r) - V_1(r) = 0 \quad ; \quad (2.1)$$

r_* must be complex since adiabatic potential curves of the same symmetry do not cross. The probability amplitude for the transition is the exponential of the classical action along this trajectory,

$$e^{i\Phi/\hbar} \quad ; \quad (2.2)$$

since the trajectory is complex valued--because it must pass through (or around) the complex crossing point--the action Φ is complex, so that the transition probability is

$$|e^{i\Phi/\hbar}|^2 = \exp(-2\text{Im}\Phi/\hbar) \quad . \quad (2.3)$$

This exponentially damped form for the non-adiabatic transition probability is reminiscent of a tunneling probability, and such transitions actually emerge in Miller and George's theory^{8,9} as a "classically forbidden" process, a generalized kind of tunneling.

By taking account of conservation of angular momentum--the orbital angular momentum of relative translational motion--atom-atom collisions reduce to one dimensional dynamical systems. The classical trajectories of the system are thus given explicitly by quadrature: the action integral along a trajectory is a radial phase integral,

$$\Phi(\ell) = \int dr \{2m [E - V(r)] - \ell^2/r^2\}^{1/2} \quad , \quad (2.4)$$

where ℓ (replaced by $\ell + 1/2$ in actual calculations) is the orbital angular momentum. If r_0 , the real part of the complex crossing point

$$r_0 \equiv \text{Re}(r_*) \quad , \quad (2.5)$$

is classically accessible on both adiabatic potentials (including the centrifugal potential)--i.e., if

$$V_i(r_0) + \ell^2/2mr_0^2 > E \quad , \quad (2.6)$$

$i = 1, 2$ --then the radial trajectory actually passes the crossing

region twice, once on the way in and once on the way out. Therefore the net amplitude, or S-matrix element, for the $1 \rightarrow 2$ transition is the sum of two terms similar to that in Eq. (2.2) (setting $\hbar = 1$):

$$S_{2,1}(\ell) = \sqrt{p_\ell(1-p_\ell)} \exp[i\phi_{\text{in}}(\ell)] + \sqrt{p_\ell(1-p_\ell)} \exp[i\phi_{\text{out}}(\ell)] \quad (2.7)$$

$$= \sqrt{p_\ell(1-p_\ell)} \mathcal{Q}_{\text{in}}(\ell) \left(1 + e^{-\pi/2} \right)$$

where

$$\phi_{\text{in}}(\ell) = \frac{\pi}{4} - k_1 r - k_2 r + \int_{r_0}^r dr' k_1(r') + \int_{r_0}^r dr' k_2(r') + 2 \int_{r_2}^{r_0} dr' k_2(r') \quad (2.8a)$$

$$\phi_{\text{out}}(\ell) = -\frac{\pi}{4} - k_1 r - k_2 r + \int_{r_0}^r dr' k_1(r') + \int_{r_0}^r dr' k_2(r') + 2 \int_{r_1}^{r_0} dr' k_1(r') \quad (2.8b)$$

with

$$k_i(r) = \{2m [E - V_i(r)] - \ell^2/r^2\}^{1/2}$$

$$k_i = k_i(\infty) \quad (2.9)$$

where $r \rightarrow \infty$ in Eq. (2.8); r_1 and r_2 are the classical turning points on V_1 and V_2 respectively. p_ℓ in Eq. (2.7) is of the form in Eq. (2.3),

$$p_\ell = \exp [-2\text{Im}\Phi(\ell)] \quad , \quad (2.10)$$

and it is easy to show that the imaginary part of the action along the complex trajectory is

$$\begin{aligned} \text{Im}\Phi(\ell) &= \text{Im} \int_{r_0}^{r_*} dr [k_1(r) - k_2(r)] \\ &= -i \int_{r_0}^{r_*} dr \text{Re} [k_1(r) - k_2(r)] \quad . \quad (2.11) \end{aligned}$$

[Note that $-idr$ is real and positive in Eq. (2.11).] The phases $\phi_{\text{in}}(\ell)$ and $\phi_{\text{out}}(\ell)$ in equation (2.7) and (2.8) are the real parts of the action integrals along this complex trajectory. The probability factor associated with each term in Eq. (2.7) corresponds to the fact that each trajectory makes a non-adiabatic transition during one passage through the crossing region and does not do so during the other passage.

The cross section for the $1 \rightarrow 2$ transition is constructed from the S-matrix in the usual fashion:

$$\sigma_{2 \leftarrow 1} = \frac{\pi}{k_1^2} \sum_{\ell=0}^{\infty} (2\ell + 1) |s_{2,1}(\ell)|^2 \quad . \quad (2.12)$$

Because many ℓ 's contribute to the partial wave sum for atom-atom collisions, it is convenient (and essentially no approximation) to replace the sum by integral, whereby Eq. (2.12) becomes

$$\sigma_{2+1} = \int_0^{\infty} db \, 2\pi b \, P_{2,1}(b) \quad , \quad (2.13)$$

where

$$b = \ell/k_1$$

$$P_{2,1}(b) = |S_{2,1}(\ell)|^2 \quad . \quad (2.14)$$

From Eq. (2.7) one has

$$P_{2,1}(b) = 4p_\ell(1 + p_\ell) \sin^2\left(\frac{\pi}{4} + \tau\right) \quad (2.15a)$$

$$= 2p_\ell(1 - p_\ell) [1 + \sin(2\tau)] \quad (2.15b)$$

with

$$\tau = \int_{r_1}^{r_0} dr \, k_1(r) - \int_{r_2}^{r_0} dr \, k_2(r) \quad ; \quad (2.16)$$

in many cases the interference term (the second term in Eq. (2.15b)) is quenched by the impact parameter integration, so that Eq. (2.15)

effectively becomes the classical result

$$P_{2,1}(b) = 2p_\ell(1 - p_\ell) \quad (2.17)$$

Eq. (2.7) applies only if r_0 is classically accessible on both adiabatic potential curves (i.e., $r_1, r_2 < r_0$); if it is classically accessible on neither ($r_1, r_2 > r_0$), then the transition must proceed by tunneling. In this case the transition involves only one complex trajectory, and the S-matrix element is thus given by

$$S_{2,1}(\ell) = \exp [i\Phi(\ell)] \quad (2.18)$$

where

$$\Phi(\ell) = -k_1 r - k_2 r + \int_{r_*}^r dr' k_1(r') + \int_{r_*}^r dr' k_2(r') \quad (2.19)$$

or

$$\begin{aligned} \Phi(\ell) = & -k_1 r - k_2 r + \int_{r_1}^r dr' k_1(r') + \int_{r_2}^r dr' k_2(r') \\ & - i \int_{r_*}^{r_1} dr' K_1(r') + i \int_{r_*}^{r_2} dr' K_2(r') \quad , \quad (2.20) \end{aligned}$$

where $r \rightarrow \infty$, and where

$$K_1(r) = \{2m [V_1(r) - E] + \ell^2/r^2\}^{1/2} \quad (2.21)$$

The transition probability is then given by

$$P_{2,1}(b) = \exp [-2\text{Im}\Phi(\ell)] \quad (2.22)$$

and from Eq. (2.20) one finds

$$\begin{aligned} \text{Im}\Phi(\ell) &= \int_{r_0}^{r_2} dr K_2(r) - \int_{r_0}^{r_1} dr K_1(r) \\ &= i \int_{r_0}^{r_*} dr' \text{Im} [K_2(r) - K_1(r)] \quad (2.23) \end{aligned}$$

For the intermediate situation that r_0 is classically accessible on the lower potential V_1 but inaccessible on the upper potential V_2 --i.e., $r_1 < r_0 < r_2$ --one needs a uniform semiclassical expression which interpolates between Eqs. (2.7)-(2.8) and Eqs. (2.18)-(2.22). This is not difficult, however, and is described in the Appendix.

At sufficiently high collision energy it is possible to simplify the above expressions. With regard to Eq. (2.11), for example, note that

$$\begin{aligned} k_1(r) - k_2(r) &= [k_1(r)^2 - k_2(r)^2] / [k_1(r) + k_2(r)] \\ &= \frac{2m}{\hbar^2} \Delta V(r) / [k_1(r) + k_2(r)] \\ &\approx \Delta V(r) / \hbar \bar{v} \quad (2.24) \end{aligned}$$

where

$$\bar{v} = \frac{\hbar}{2m} [k_2(r_0) + k_1(r_0)] \quad (2.25)$$

is the average velocity at r_0 . Eq. (2.11) then becomes

$$\text{Im}\phi(\ell) = (\hbar\bar{v})^{-1} (-i) \int_{r_0}^{r_*} dr \Delta V(r) \quad (2.26)$$

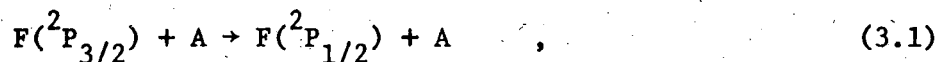
An even cruder, but simpler (and therefore more popular) high energy approximation results if one takes the average velocity \bar{v} to be the free particle velocity

$$\bar{v} \approx v(1 - b^2/r_0^2)^{1/2}, \quad (2.27)$$

where $v = (2E/m)^{1/2}$ is the asymptotic velocity. At high collision energy it is also necessary to modify the expression for p_ℓ (see Section IV).

III. ADIABATIC POTENTIAL CURVES.

To describe the fine-structure transition



where A is a rare gas atom, one needs the Born-Oppenheimer potential curves which take account of spin-orbit coupling in the F atom. A full, ab initio calculation including spin-orbit interactions is a considerable undertaking, but the following simplified approach is usually reasonably accurate.

The Born-Oppenheimer electronic Hamiltonian (i.e., the full Hamiltonian minus the kinetic energy of the nuclei) is of the form

$$H = H_{\text{stat}} + H_{\text{SO}} \quad , \quad (3.2)$$

where H_{stat} is an ordinary electrostatic Hamiltonian (electronic kinetic energy plus the coulomb interactions of electrons and nuclei) and H_{SO} a spin-orbit operator for an isolated F atom:

$$H_{\text{SO}} = -\left(\frac{2}{3} \Delta\right) \underline{L} \cdot \underline{S} \quad , \quad (3.3)$$

where \underline{L} and \underline{S} are electronic orbital and spin operators for the F atom and $\Delta = 404 \text{ cm}^{-1}$ is the fine-structure splitting in an

isolated F atom. If $|j, m_j\rangle$ denotes states of total electronic angular momentum and its z-projection, then it is not difficult to show that the matrix representation of the electrostatic Hamiltonian in this basis is

$$\langle j', m_j' | H_{\text{stat}} | j, m_j \rangle = \delta_{m_j', m_j} \sum_{m_\ell} C(1 \frac{1}{2} j'; m_\ell, m_j - m_\ell) C(1 \frac{1}{2} j; m_\ell, m_j - m_\ell) v_{|m_\ell|} \quad (3.4)$$

where the C's are Clebsch-Gordan coefficients and $v_{|m_\ell|}$ are the eigenvalues of the electrostatic Hamiltonian; i.e., $v_0(r)$ and $v_1(r)$ are the Σ and Π potential curves, respectively, for F - A obtained by ignoring spin-orbit coupling. The spin-orbit Hamiltonian is completely diagonal in this representation:

$$\begin{aligned} \langle j', m_j' | H_{\text{SO}} | j, m_j \rangle &= -\frac{\Delta}{3} [j(j+1) - 1(1+1) - \frac{1}{2}(\frac{1}{2} + 1)] \delta_{j', j} \delta_{m_j', m_j} \\ &= -\frac{\Delta}{3} [j(j+1) - \frac{11}{4}] \delta_{j', j} \delta_{m_j', m_j} \quad (3.5) \end{aligned}$$

The total Hamiltonian is thus completely diagonal in m_j and is designated as

$$H_{j', j}^{(m_j)} \quad (3.6)$$

For $m_j = \frac{3}{2}$, j and j' can only take on the value $\frac{3}{2}$, so that the matrix is one dimensional. Thus

$$H_{\frac{3}{2}, \frac{3}{2}} \begin{pmatrix} \frac{3}{2} \\ \frac{3}{2} \end{pmatrix} = v_{\Pi} - \frac{\Delta}{3} \quad (3.7)$$

is one of the eigenvalues. For $m_j = 1/2$, j and j' can take on values $1/2$ and $3/2$, so $H^{(1/2)}$ is two dimensional with elements

$$H_{\frac{1}{2}, \frac{1}{2}} \begin{pmatrix} \frac{1}{2} \\ \frac{1}{2} \end{pmatrix} = \frac{1}{3} v_{\Sigma} + \frac{2}{3} v_{\Sigma} + \frac{2}{3} \Delta \quad (3.8a)$$

$$H_{\frac{3}{2}, \frac{3}{2}} \begin{pmatrix} \frac{1}{2} \\ \frac{1}{2} \end{pmatrix} = \frac{2}{3} v_{\Sigma} + \frac{1}{3} v_{\Sigma} - \frac{1}{3} \Delta \quad (3.8b)$$

$$H_{\frac{1}{2}, \frac{3}{2}} \begin{pmatrix} \frac{1}{2} \\ \frac{1}{2} \end{pmatrix} = H_{\frac{3}{2}, \frac{1}{2}} \begin{pmatrix} \frac{1}{2} \\ \frac{1}{2} \end{pmatrix} = -\frac{\sqrt{2}}{3} (v_{\Pi} - v_{\Sigma}) \quad ; \quad (3.8c)$$

the eigenvalues of this 2 by 2 matrix are easily found to be

$$V(r) = \frac{1}{2}(v_{\Sigma} + v_{\Pi}) + \frac{1}{6}\Delta \pm \frac{1}{2}[(v_{\Pi} - v_{\Sigma})^2 + \frac{2}{3}\Delta(v_{\Pi} - v_{\Sigma}) + \Delta^2]^{\frac{1}{2}}. \quad (3.9)$$

Since

$$\lim_{r \rightarrow \infty} v_{\Sigma}(r) = \lim_{r \rightarrow \infty} v_{\Pi}(r) = 0 \quad , \quad (3.10)$$

these two eigenvalues asymptotically become

$$\frac{1}{6}\Delta \pm \frac{1}{2}\Delta = \frac{2}{3}\Delta, -\frac{1}{3}\Delta, \quad (3.11)$$

the energy levels of $^2P_{1/2}$ and $^2P_{3/2}$ F atoms, respectively, referred to atom A and the "center of gravity" of the $F(^2P)$ manifold.

The $^2P_{3/2} \rightarrow ^2P_{1/2}$ transition thus takes place within the $m_j = 1/2$ block of the Hamiltonian matrix. If $V_1(r)$ and $V_2(r)$ denote the two adiabatic potential curves given by Eq. (3.9), then the complex crossing point is the root of

$$\begin{aligned} \Delta V(r) &= \{ [v_{\Pi}(r) - v_{\Sigma}(r)]^2 + \frac{2}{3}\Delta [v_{\Pi}(r) - v_{\Sigma}(r)] + \Delta^2 \}^{1/2} \\ &= 0, \end{aligned} \quad (3.12)$$

which is also equivalent to

$$v_{\Pi}(r) - v_{\Sigma}(r) = \Delta \exp \left[\pm i \cos^{-1} \left(-\frac{1}{3} \right) \right]. \quad (3.13)$$

If Δ is fairly large, as it is in the present case, then the crossing point will occur at sufficiently small r for the $\Sigma - \Pi$ splitting to be determined by electron exchange interactions.

In such cases the splitting is often well approximated as a simple exponential function

$$v_{\Pi}(r) - v_{\Sigma}(r) = A e^{-\lambda r} \quad , \quad (3.14)$$

and with this form one sees that the roots of Eq. (3.13) are

$$r_{*} = \lambda^{-1} \left[\ln(A/\Delta) \pm i \cos^{-1} \left(-\frac{1}{3} \right) \right] \quad . \quad (3.15)$$

With the $\Sigma - \Pi$ splitting assumed to have the form in Eq. (3.14) it is possible to evaluate the imaginary part of the action interval explicitly within the high energy approximation:

$$\text{Im}\Phi(\ell)/\hbar = (\hbar v)^{-1} (-i) \int_{r_0}^{r_*} dr \Delta V(r) \quad , \quad (3.16)$$

and with Eq. (3.14) and Eq. (3.15) this becomes

$$\begin{aligned} \text{Im}\Phi(\ell)/\hbar &= \frac{\Delta}{\hbar v \lambda} \int_0^{\cos^{-1}(-\frac{1}{3})} dx \left[e^{2ix} + \frac{2}{3} e^{ix} + 1 \right]^{1/2} \\ &= \frac{\Delta}{\hbar v \lambda} \left(\frac{2\pi}{3} \right) \quad , \quad (3.17) \end{aligned}$$

so that the high energy approximation to the non-adiabatic transition probability is

$$\begin{aligned} p_{\ell} &= \exp [- 2\text{Im}\Phi(\ell)/\hbar] \\ &= \exp \left(- \frac{4\pi}{3} \frac{\Delta}{\hbar v \lambda} \right) \quad , \quad (3.18) \end{aligned}$$

a result obtained by Nikitin.¹ At energies so large that p_ρ is not small compared to 1, however, it is necessary to use a renormalized version which takes proper account of crossing points further from the real axis; this has been discussed by Nikitin,¹² and for the present case is

$$p_\rho = [\exp(-2\text{Im}\Phi) - \exp(-3\text{Im}\Phi)]/[1 - \exp(-3\text{Im}\Phi)] \quad (3.19)$$

In order to apply the semiclassical expressions summarized in Section II, either exactly or within the high energy approximation, it is necessary to analytically continue the adiabatic potential functions $V_1(r)$ and $V_2(r)$, first in order to find the complex root of Eq. (2.1) and then in order to evaluate the integrals in Eq. (2.11) or Eq. (2.26); only $\Delta V(r)$ must be analytically continued in order to compute the approximate result [(Eq. 2.26)], whereas both $V_1(r)$ and $V_2(r)$ are separately required in the more correct version, Eq. (2.11). It is often possible to fit the adiabatic potential functions to simple analytic forms, as was discussed above, and in such cases the analytic continuation of the adiabatic potential curves to complex r is trivial. Other simple parameterized models often used for $\Delta V(r)$ are the Landau-Zener model^{11,13}

$$\Delta V(r) = [a^2 + f^2(r - r_0)^2]^{1/2} \quad (3.20)$$

and the Demkov model¹⁴

$$\Delta V(r) = [\Delta^2 + 4A^2 e^{-2\lambda r}]^{1/2} \quad (3.21)$$

where a , f , Δ , A , and λ are constant.

In general, however, the analytic continuation of $V_1(r)$ and $V_2(r)$ is not so straight-forward, particularly so if they are the numerical output of a Born-Oppenheimer eigenvalue calculation. In many cases one may be able to fit the potential curves calculated for real r to a simple functional form and then use this analytic fit to determine the potential also for complex r . One would expect this to be reliable for complex values of r not too far from the real axis.

The most general way of analytically continuing the potential curves to complex values of r is to return to the electronic secular equation from which they come; i.e., the adiabatic potential curves $V_i(r)$ are the roots of the secular equation

$$\det |H_{ij}(r) - V(r) \delta_{ij}| = 0 \quad (3.22)$$

$H_{ij}(r)$ is the $N \times N$ matrix of the electronic Hamiltonian in an N -dimensional electronic basis set which depends parametrically on the nuclear separation r ; these matrix elements, being combinations of coulomb and exchange integrals, are manifestly analytic functions of r and can be directly evaluated for complex r . The

secular determinant is a Nth order polynomial in V, and the N eigenvalues are the roots of this polynomial. For N = 2, for example, one can find the two roots of the quadratic equation explicitly;

$$V(r) = \frac{1}{2}[H_{11}(r) + H_{22}(r)] \pm \left\{ \frac{1}{4}[H_{11}(r) - H_{22}(r)]^2 + H_{12}(r)^2 \right\}^{1/2}. \quad (3.23)$$

For $N > 2$ it is not easy to write down the N roots of Eq. (3.22) explicitly, but there are many operational procedures for finding them. The important point is that the eigenvalues $\{V_i(r)\}$ are an algebraic function of the electronic matrix elements $H_{ij}(r)$. One thus analytically continues $H_{ij}(r)$ to complex values of r by inspection and obtains $\{V_i(r)\}$ by finding the roots of Eq. (3.22); if the appropriate "eigenvalue finder" is used, then the only changes that need be made in the computer program is simply to declare all quantities, H_{ij} and V, to be the COMPLEX Fortran variables and proceed with the same algebraic manipulations as if one were finding real eigenvalues. George and Morokuma¹⁵ have carried out such calculations.

Another interesting point is that the N different adiabatic potential curves $\{V_i(r)\}$ are actually the N different branches, or Riemann sheets of the same analytic function. For $N = 2$, for example, this is seen explicitly in Eq. (3.23), where the two eigenvalues result because of the double-valued character

of the square root function. Similarly, there are three roots to a three by three secular equation because of the triple-valuedness of the cube root function, and in general the N roots of the secular equation are a result of the N -fold multivaluedness of the N th root function. In truth, therefore, there is just one adiabatic potential energy function, but it happens to be multivalued; within the Stueckelberg model transitions between different adiabatic electronic states occur by complex-valued classical trajectories that go around branch points of the multivalued potential function and thus change from one Riemann sheet (i.e., electronic state) to another.

Another interesting feature of this semiclassical description of nonadiabatic transitions is that nowhere do Born-Oppenheimer coupling terms enter into the picture explicitly; the transition probability given by Eq. (2.7) - (2.15), for example, involves only the adiabatic potential curves $V_i(\mathbf{r})$. This means that all information regarding the nonadiabatic coupling terms which is required for the semiclassical model is contained implicitly in the analytic structure of the (multivalued) adiabatic potential function. This point will be illustrated more fully with the example discussed in Section IV.

IV. RESULTS FOR F + Xe.

Figure 1 shows the difference of the $^2\Sigma$ and $^2\Pi$ states of Xe - F as calculated by Liskow, Schaefer, Bagus, and Liu.¹⁶

Over the range of interest the potential difference is fit well by a single exponential, i.e., by Eq. (3.14), where the "best fit" parameters are

$$A = 48.2 \text{ hartrees}$$

$$\lambda = 1.65 a_0^{-1}.$$

The complex crossing point is thus given by Eq. (3.15), which with these values of the parameters is

$$r_* = [6.15 \pm i(1.16)] a_0 \quad (4.1)$$

Figure 2 shows the impact parameter dependence of the transition probability computed from the "exact" version of the semiclassical expressions [Eqs. (2.7) - (2.16)] at a typical "high" collision energy (1.0 eV); the inset shows more detail of the large impact parameter region where the transition takes place by tunneling [Eq. (2.18)-(2.23)]. The dashed line shows the "classical" result [Eq. (2.17)] obtained by discarding the interference term in Eq. (2.15b). It is clear from the figure that the tunneling contribution is negligible at this energy and that there are enough oscillations in the transition probability for the impact parameter integration to quench the interference term. It is also clear, however, that interference

effects (Stuckelberg oscillations) should be quite prominent in the inelastic differential cross section. Figure 3 shows a similar plot for a "low" collision energy (0.1 eV), and one sees that the omission of interference is less justifiable here. Impact parameter averages cover a multitude of sines, however, and even here the cross section obtained from the "classical" probability function in Fig. 3 is in error by only 20%; by 0.2 eV the error drops to 10%. Again, the classical version of the theory, i.e., the neglect of interference, would be much less satisfactory for the differential cross section.

Figure 4 shows the cross section for the ${}^2P_{3/2} \rightarrow {}^2P_{1/2}$ excitation of F atom as a function of relative collision energy. [The cross sections shown in this paper include a sum and average over the m_j -components of the electronic angular momentum of the F atom; since only the $m_j = \pm \frac{1}{2}$ components give rise the transition, a factor of $\frac{1}{2}$ must be supplied to the cross section formulae of Section II when considering the excitation process. This factor of $\frac{1}{2}$ is included in all displayed cross sections.] The dashed curve is the result of the "exact" version of the theory, and the solid curve the classical version which omits interference. One sees that only a slight oscillatory structure survives the impact parameter average, and it would probably be unobservable under realistic experimental conditions.

Although there are other effects which must be taken into account at high (non-thermal) collision energies--primarily the

coriolis interaction--it is of practical interest to see at what energy the simpler high energy approximation to the semiclassical expressions becomes valid. Utilizing the renormalized p_ρ given by Eq. (3.19) and taking \bar{v} as the free particle velocity [Eq. (2.27)], the cross section is given by (including the statistical factor of $\frac{1}{2}$)

$$\sigma_{\frac{1}{2} \leftarrow \frac{3}{2}} = \left(\frac{1}{2}\right) \int_0^{r_0} db (2\pi b)^2 (e^{-2\xi} - e^{-3\xi}) (1 - e^{-2\xi}) (1 - e^{-3\xi})^{-2} \quad (4.2)$$

$$\xi = \frac{2}{3} \frac{\pi \Delta}{\hbar v \lambda} \left(1 - \frac{b^2}{r_0^2}\right)^{-1/2} \quad (4.3)$$

where the interference term and the tunneling contribution has been discarded. A suitable change of integration variables cast this into a more useful form:

$$\sigma_{\frac{1}{2} \leftarrow \frac{3}{2}} = \frac{2}{9\pi} r_0^2 f[(E/E_0)^{1/2}] \quad (4.4)$$

where

$$E_0 = \frac{1}{2} \mu \left(\frac{\pi \Delta}{\hbar \lambda}\right)^2 \quad (4.5)$$

and $f(x)$ is the dimensionless function (a reduced cross section) of the dimensionless variable x (a reduced velocity):

$$f(x) = \int_{\frac{2}{3}}^{\infty} dy \, 4y^{-3} (e^{-2y/x} - e^{-3y/x}) (1 - e^{-2y/x}) \times (1 - e^{-3y/x})^{-2} \quad (4.6)$$

One can show that

$$f(x) \sim 1 - \frac{2}{3} x^{-1}, \quad x \rightarrow \infty$$

$$\sim \frac{27}{4} x \exp\left(-\frac{4}{3x}\right), \quad x \rightarrow 0 \quad ; \quad (4.7)$$

Figure 5 shows this function $f(x)$. For the present case of Xe - F the characteristic cross section has the value

$$\frac{2}{9\pi} r_0^2 = 26.4 a_0^2 = 7.4 \text{ \AA}^2, \quad (4.8)$$

and the characteristic energy E_0 of Eq. (4.5) is

$$E_0 = 5.06 \text{ eV} \quad (4.9)$$

Figure 6 shows the reduced cross section $f(x)$ in more detail in the low energy region, compared to the "classical" results of Fig. 4 (divided by $\frac{2}{9\pi} r_0^2$). Above 0.5 eV collision energy one sees that the high energy approximation is essentially exact, but below 0.5 eV it is important to take account of the full dynamics correctly.

In order to gain some insight into the nature of the semiclassical description of nonadiabatic transitions it is interesting to look explicitly at the nonadiabatic coupling which would be required if the coupled channel Schroedinger equation were to be solved in the adiabatic representation. Apart from constants the interaction which couples adiabatic states 1 and 2 is

$$\int dq \Psi_1(q;r) \frac{\partial \Psi_2(q;r)}{\partial r} \quad , \quad (4.10)$$

where q denotes all electronic coordinates and $\{\Psi_i\}$ are adiabatic electronic wavefunctions. If one ignores nonadiabatic effects in the $^2\Sigma$ and $^2\Pi$ electronic states themselves, then Ψ_1 and Ψ_2 are of the form

$$\Psi_i(q;r) = C_{i1}(r) \chi_1(q) + C_{i2}(r) \chi_2(q) \quad , \quad (4.11)$$

where χ_1 and χ_2 are the Σ and Π electronic states; the r - dependent coefficient matrix is the unitary matrix which diagonalizes the two by two Hamiltonian matrix of Eq. (3.8). It is then a simple matter to show that

$$\int dq \Psi_1(q;r) \frac{\partial \Psi_2(q;r)}{\partial r} = \frac{\Delta H(r) H'_{12}(r) - \Delta H'(r) H_{12}(r)}{\Delta H(r)^2 + 4H_{12}(r)^2} \quad ,$$

where

$$\Delta H(r) = H_{22}(r) - H_{11}(r) \quad . \quad (4.12)$$

This quantity is shown in Figure 7; it takes on its maximum precisely at r_0 , the real part of the complex crossing point, and this is the quantum mechanical manifestation of the fact that nonadiabatic transitions are localized in the region about r_0 . Even though coupling terms such as these are not needed for the semiclassical theory, the analytic structure of the adiabatic potential function--which is needed--effectively has this information contained in it.

V. RESULTS FOR F + H⁺

While the work on Xe + F was in progress Mies'⁴ paper on H⁺ + F appeared and thus provided the possibility of a direct comparison of the semiclassical model with a quantum mechanical coupled-channel calculation. Such comparisons for atom-atom collision systems will be important for establishing the validity of the semiclassical model since this will not be possible in the case of atom-diatom collisions.

We at first attempted to use Mies' analytic fits¹⁷ to the $^2\Sigma$ and $^2\Pi$ states¹⁸ of HF⁺ and find the roots of Eq. (3.12). This was not possible, however, for these analytic fits were too structured--similar to high order Lagrangian interpolation--so that their analytic continuation into the complex plane was unstable. If the $\Sigma - \Pi$ difference itself is plotted on a semilog scale (as shown in Figure 8), however, one sees a rather simple functional form. Over the significant range of internuclear distance the logarithm of the difference is fit well by a quadratic, implying a gaussian fit to the $\Sigma - \Pi$ splitting:

$$v_{\Sigma}(r) - v_{\Pi}(r) = A e^{-\lambda r + \gamma r^2} \quad , \quad (5.1)$$

where the parameters are

$$A = 0.4676 \text{ hartrees}$$

$$\lambda = 1.001 a_0^{-1}$$

$$\gamma = 0.03814 a_0^{-2}$$

Since the Π potential curve lies below the Σ curve in this case,¹⁸
 Eq. (3.13) for the complex crossing point is replaced by

$$v_{\Sigma}(r) - v_{\Pi}(r) = \Delta \exp[\pm i \cos^{-1}(\frac{1}{3})] \quad , \quad (5.2)$$

and with the functional form in Eq. (5.1) one finds the root
 of Eq. (5.2) to be

$$r_{*} = \frac{\lambda}{2\gamma} \left[1 - \left(1 - \frac{4\gamma}{\lambda} r_{*}^{(0)} \right)^{1/2} \right] \quad ,$$

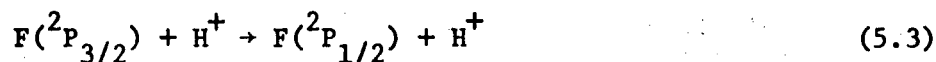
where

$$r_{*}^{(0)} = \lambda^{-1} \left[\ln(A/\Delta) \pm i \cos^{-1}(\frac{1}{3}) \right] \quad ;$$

with the above parameters this gives

$$r_{*} = [7.25 \pm i (2.75)] a_0 \quad .$$

Figure 9 shows the cross section for



as a function of the relative collision energy; the individual
 points are the values of Mies' quantum mechanical calculations,⁴

and although not spectacular, the agreement is seen to be reasonable. Because of the strong attractive potential wells in both the Σ and Π states¹⁸ of $H^+ - F$, the present semiclassical model--which ignores the coriolis interaction--is not expected to be as applicable here as it is for F plus closed-shell neutral atoms and molecules for which the interaction is predominantly repulsive.

VI. CONCLUDING REMARKS.

The semiclassical model for non-adiabatic electronic transitions provides an interesting and simple picture of such processes: the transition takes place along a classical trajectory which passes through a complex crossing point of the adiabatic potential curves. The particularly interesting aspect of the examples presented in this paper is that the adiabatic potential curves have no "avoided intersection" for real r , so that it might have been thought that no such semiclassical treatment was possible. As has been seen, however, complex crossing points exist even for these cases, and the semiclassical theory seems to provide a good description of the non-adiabatic process.

For the Xe - F example the cross section is small at thermal energy, reaching only $\sim 0.1 \text{ \AA}^2$ at a collision energy of 0.5 eV. If the cross section for $F + H_2^{6,7}$ were of a similar magnitude, then for thermal energy collisions the best zero-th order approximation would be to assume that no non-adiabatic transitions occur. In the thermal energy regime below 0.5 eV it is important to include the full heavy particle dynamics of the crossing encounter, although the high energy approximation is accurate above 0.5 eV.

For H^+ - F the cross section is much larger, which is perhaps expected on account of the charged species. This example also shows some of the practical difficulties that can arise when applying the semiclassical theory, namely the necessity of analytically continuing the adiabatic potential curves into the complex plane. If the potential curves have a simple shape, as for Xe - F,

then it should be possible to fit them to simple functional forms and extrapolate these analytic fits to complex r ; if the required fit is too structured, however, this approach may not be possible. The most general solution to this problem is to calculate the potential curves directly in the complex plane, as George and Morokuma¹⁵ have done, but this of course adds to the overall complexity of the calculation. Whether this kind of practical difficulty proves to be common or rare will not be known until more examples have been studied.

In conclusion, the semiclassical model for non-adiabatic electronic transitions appears to be a useful technique for describing these processes, particularly so at thermal energy where it is important to incorporate the full heavy particle dynamics. Since all dynamics is treated classically, only the superposition principle of quantum mechanics being included, it is possible to use the model in conjunction with numerically computed classical trajectories for more complex systems, e.g., atom-diatom collisions, and we anticipate future work in this direction.

APPENDIX: A UNIFORM APPROXIMATION FOR WEAK TRANSITIONS

Referring to Figure 10, Eq. (2.7) - (2.8) and Eq. (2.18) - (2.19) are the semiclassical approximation to the S-matrix for $E \gg E_2$ and $E \ll E_1$, respectively. Since the effective potentials sketched in Fig. 10 increase with increasing impact parameter, E_1 and E_2 do also, so that one would like to have an expression which is valid uniformly for $E > E_2$, $E_1 < E < E_2$, and $E < E_1$. Here we show how such an expression can be constructed for the near-adiabatic limit ($|S_{2,1}|^2 \ll 1$) which is usually the situation at low energy. Rather than being a uniform asymptotic approximation in the rigorous sense of the word--which we cannot prove--the result has more the status of a useful interpolation formula.

By making use of the known asymptotic expressions for the Airy function¹⁹--namely

$$\text{Ai}(-z) \sim \pi^{-1/2} z^{-1/4} \sin\left(\frac{\pi}{4} + \frac{2}{3} z^{3/2}\right) \quad (\text{A.1})$$

$$\text{Ai}(\bar{z}) \sim \frac{1}{2} \pi^{-1/2} \bar{z}^{-1/4} \exp\left(-\frac{2}{3} \bar{z}^{3/2}\right), \quad (\text{A.2})$$

for z, \bar{z} real and $\gg 1$ --one can easily show that Eq. (2.7) and (2.18) are equivalent (in the near-adiabatic limit) to

$$S_{2,1} = \exp\left[-ik_1 r - ik_2 r + i \int_{r_1}^r dr' k_1(r') + i \int_{r_2}^r dr' k_2(r')\right. \\ \left. + i \int_{r_0}^{r_*} dr' k_1(r') - i \int_{r_0}^{r_*} dr' k_2(r')\right] 2\pi^{1/2} z^{1/4} \text{Ai}(-z) \quad (\text{A.3a})$$

$$z = \left\{ \frac{3}{2} \left[\int_{r_1}^{r_0} dr k_1(r) - \int_{r_2}^{r_0} dr k_2(r) \right] \right\}^{2/3} \quad (\text{A.3b})$$

for $E > E_2$, and

$$S_{2,1} = \exp[-ik_1 r - ik_2 r + i \int_{r_1}^r dr' k_1(r') + i \int_{r_2}^r dr' k_2(r')] \\ - \int_{r_0}^{r_*} dr' K_1(r') + \int_{r_0}^{r_*} dr' K_2(r')] \quad 2\pi^{1/2} \bar{z}^{-1/4} \text{Ai}(\bar{z}) \quad (\text{A.4a})$$

$$\bar{z} = \left\{ \frac{3}{2} \left[\int_{r_0}^{r_2} dr K_2(r) - \int_{r_0}^{r_1} dr K_1(r) \right] \right\}^{2/3} \quad (\text{A.4b})$$

for $E < E_1$, respectively. Eqs. (A.3) and (A.4) are so similar that at first glance one might think that they are the desired uniform expression as they stand. For this to be the case it would be necessary for Eq. (A.4) to result from Eq. (A.3), for example, as E is decreased continuously from above E_2 to below E_1 ; i.e., Eq. (A.3) and (A.4) should be the analytic continuation of each other. If for $E < E_n$ one chooses

$$k_n(r) = i K_n(r) \quad ,$$

then the correct exponential factor is obtained for Eq. (A.4), and for $E < E_1$ the variable z of Eq. (A.3b) becomes

$$z = \bar{z} i^{2/3} \quad ,$$

where $\bar{z} = |z|$ is given by Eq. (A.4b). The $\frac{2}{3}$ - root function is triple-valued --

$$i^{2/3} = e^{i\pi/3}, e^{-i\pi/3}, \text{ or } -1$$

-- and to obtain the correct result for Eq. (A.4a) it is clear that one must choose the branch $i^{2/3} = -1$. The problem, however, is that as E is decreased continuously from above E_2 to below E_1 , a continuous variation of z--which is clearly necessary to have a uniformly valid expression--leads to the branch $i^{2/3} = e^{i\pi/3}$ or $e^{-i\pi/3}$, not the desired branch $i^{2/3} = -1$. Analytic continuation of Eq. (A.3) to values of E below E_1 , therefore, does not lead to the correct result, Eq. (A.4), and is thus not the desired uniform expression.

To remedy the situation one invokes the identity¹⁹

$$\text{Ai}(-z) = e^{-i\pi/3} \text{Ai}(ze^{-i\pi/3}) + e^{i\pi/3} \text{Ai}(ze^{i\pi/3}) \quad , \quad (\text{A.5})$$

for the Airy function in Eq. (A.3a). Now as E is decreased to values below E_1 one chooses z to be

$$z = \bar{z} e^{i\pi/3}$$

for the first term in Eq. (A.5), and

$$z = \bar{z} e^{-i\pi/3}$$

for the second term in Eq. (A.5). Since

$$e^{-i\pi/3} + e^{i\pi/3} = 1 \quad ,$$

The RHS of Eq. (A.5) becomes $\text{Ai}(\bar{z})$, so that Eq. (A.4) is obtained.

To summarize, the desired uniform expression is

$$\begin{aligned}
 S_{2,1} = & \exp[-ik_1 r - ik_2 r + i \int_{r_1}^r dr' k_1(r') + i \int_{r_2}^r dr' k_2(r') \\
 & + i \int_{r_0}^{r_*} dr' k_1(r') - i \int_{r_0}^{r_*} dr' k_2(r')] 2\pi^{1/2} (z_1 z_2)^{1/8} \\
 & [e^{-i\pi/3} \text{Ai}(z_1 e^{-i\pi/3}) + e^{i\pi/3} \text{Ai}(z_2 e^{i\pi/3})] , \quad (\text{A.6})
 \end{aligned}$$

where $r \rightarrow \infty$; for $E > E_2$, $z_1 = z_2 = z$, z real and positive, defined by Eq. (A.3b). For $E < E_2$, z_1 and z_2 are complex, being different branches of the multivalued function z ; z_1 is the branch which becomes $\bar{z} e^{i\pi/3}$ for $E < E_1$, and z_2 is the branch which becomes $\bar{z} e^{-i\pi/3}$. Via Eq. (A.6), therefore, Eqs. (A.3) and (A.4) are now seen to be analytic continuations of each other, and one also has a well-behaved expression for the intermediate region $E_1 < E < E_2$.

REFERENCES.

- * Supported in part by the U. S. Atomic Energy Commission, and by the National Science Foundation under grant GP-34199X.
- † Camille and Henry Dreyfus Teacher-Scholar.
1. E. E. Nikitin, Comments Atom. Mol. Phys. 3, 7 (1971); E. I. Dashevskaya, E. E. Nikitin, and A. I. Reznikov, J. Chem. Phys. 53, 1175 (1970); E. E. Nikitin, Opt. Spektrosk. 19, 91 (1965); E. E. Nikitin, J. Chem. Phys. 43, 744 (1965).
 2. (a) R. H. G. Reid and A. Dalgarno, Chem. Phys. Lett. 6, 85 (1970); (b) R. E. Johnson, J. Phys. B 3, 539 (1970).
 3. F. Masnou-Seeuws, J. Phys. B 3, 1437 (1970); F. Masnou-Seeuws and E. Roueff, Chem. Phys. Lett. 16, 593 (1972).
 4. F. H. Mies, Phys. Rev. A 7, 942, 957 (1973).
 5. R. H. G. Reid, J. Phys. B 6, 2018 (1973).
 6. D. G. Truhlar, J. Chem. Phys. 56, 3189 (1972); J. T. Muckermann and M. D. Newton, ibid. 3191.
 7. J. C. Tully, J. Chem. Phys. 60, 0000 (1974).
 8. W. H. Miller and T. F. George, J. Chem. Phys. 56, 5637 (1972).
 9. W. H. Miller, Adv. Chem. Phys. 25, 63 (1974).
 10. J. C. Tully and R. K. Preston, J. Chem. Phys. 55, 562 (1971).
 11. E. C. G. Stuckelberg, Helv. Phys. Acta 5, 369 (1932).
 12. E. E. Nikitin, in Chemische Elementarprozesse, eds. J. Heidberg, H. Heydtmann, and G. H. Kohlmaier, Springer, N.Y., 1968, p. 43; E. E. Nikitin, Adv. Quant. Chem. 5, 135 (1970).

13. L. D. Landau, Physik. Z. Sowjetunion U.R.S.S. 2, 46 (1932);
C. Zener, Proc. Roy. Soc. (London) A137, 696 (1932).
14. Yu. N. Demkov, Soviet Physics JETP 18, 138 (1964).
15. K. Morokuma and T. F. George, J. Chem. Phys. 59, 1959 (1973);
T. F. George and K. Morokuma, Chem. Phys. 2, 129 (1973);
Y.-W. Lin, T. F. George, and K. Morokuma, Chem. Phys. Lett.
22, 547 (1973).
16. D. Liskow, H. F. Schaefer, P. S. Bagus, and B. Liu, J. Am. Chem. Soc. 95, 4056 (1973).
17. F. Mies, private communication.
18. A. C. Wahl, P. Julienne, and M. Krauss, Chem. Phys. Lett. 11, 16 (1971).
19. M. Abramowitz and I. A. Stegun, Handbook of Mathematical Functions, NBS Appl. Math. Ser. 55, U.S. Gov. Print. Off., Washington, 1965, pp. 446-449.

FIGURE CAPTIONS.

1. The difference of the $^2\Pi$ and $^2\Sigma$ potential curves of Xe - F(2P) as a function of internuclear distance. The points are those calculated by Liskow, et al. (ref. 16), and the curve is the exponential function $A\exp(-\lambda r)$, with $\lambda = 1.65 a_0^{-1}$, $A = 48.2$ hartrees.
2. The transition probability for $\text{Xe} + \text{F}(^2P_{3/2}) \rightarrow \text{Xe} + \text{F}(^2P_{1/2})$ as a function of impact parameter at an initial collision energy of 1 eV. The solid line (including the insert) is the result of the complete semiclassical expression [Eqs. (2.10), (2.11), (2.15)] , and the dashed line the classical result [Eqs. (2.10), (2.11), (2.17)] which omits interference and tunneling.
3. Same as Figure 2 except for a collision energy of 0.1 eV.
4. The cross section for $\text{Xe} + \text{F}(^2P_{3/2}) \rightarrow \text{Xe} + \text{F}(^2P_{1/2})$ as a function of initial collision energy; the arrow indicates the threshold. The solid curve is the classical result which omits interference and tunneling, and the dashed curve the result of the complete semiclassical expressions.
5. The reduced cross section of Eq. (4.6) - (4.7) which is obtained in the high energy approximation, as a function of the reduced velocity.
6. The cross section, in units of $\frac{2}{9} \pi r_0^2$, for $\text{Xe} + \text{F}(^2P_{3/2}) \rightarrow \text{Xe} + \text{F}(^2P_{1/2})$ as a function of the reduced velocity. The solid curve is the "classical" version of the semiclassical result

(i.e., the same as the solid curve in Fig. 4), and the dashed curve is the high energy approximation to it; i.e., the dashed curve is the function $f(x)$ of Eq. (4.6) - (4.7) with $x = (E/E_0)^{1/2}$.

7. The non-adiabatic coupling matrix element for $Xe + F$, defined by Eqs. (4.10) - (4.12), as a function of internuclear distance.
8. The difference of $^2\Pi$ and $^2\Sigma$ potential curves of $H^+ - F(^2P)$ as a function of internuclear distance. The points are the calculation of Wahl et al. (ref. 18), and the solid curve the gaussian fit of Eq. (5.1).
9. The cross section for $H^+ + F(^2P_{3/2}) \rightarrow H^+ + F(^2P_{1/2})$ as a function of initial collision energy; the arrow indicates the threshold for the transition. The points are the quantum mechanical values of Mies (ref. 4).
10. A sketch of two adiabatic potential curves. r_0 is the real part of the complex crossing point; for $E > E_2$, $E_1 < E < E_2$, or $E < E_1$, r_0 is classically accessible on both potential curves, only on $V_1(r)$, or on neither potential curve, respectively.

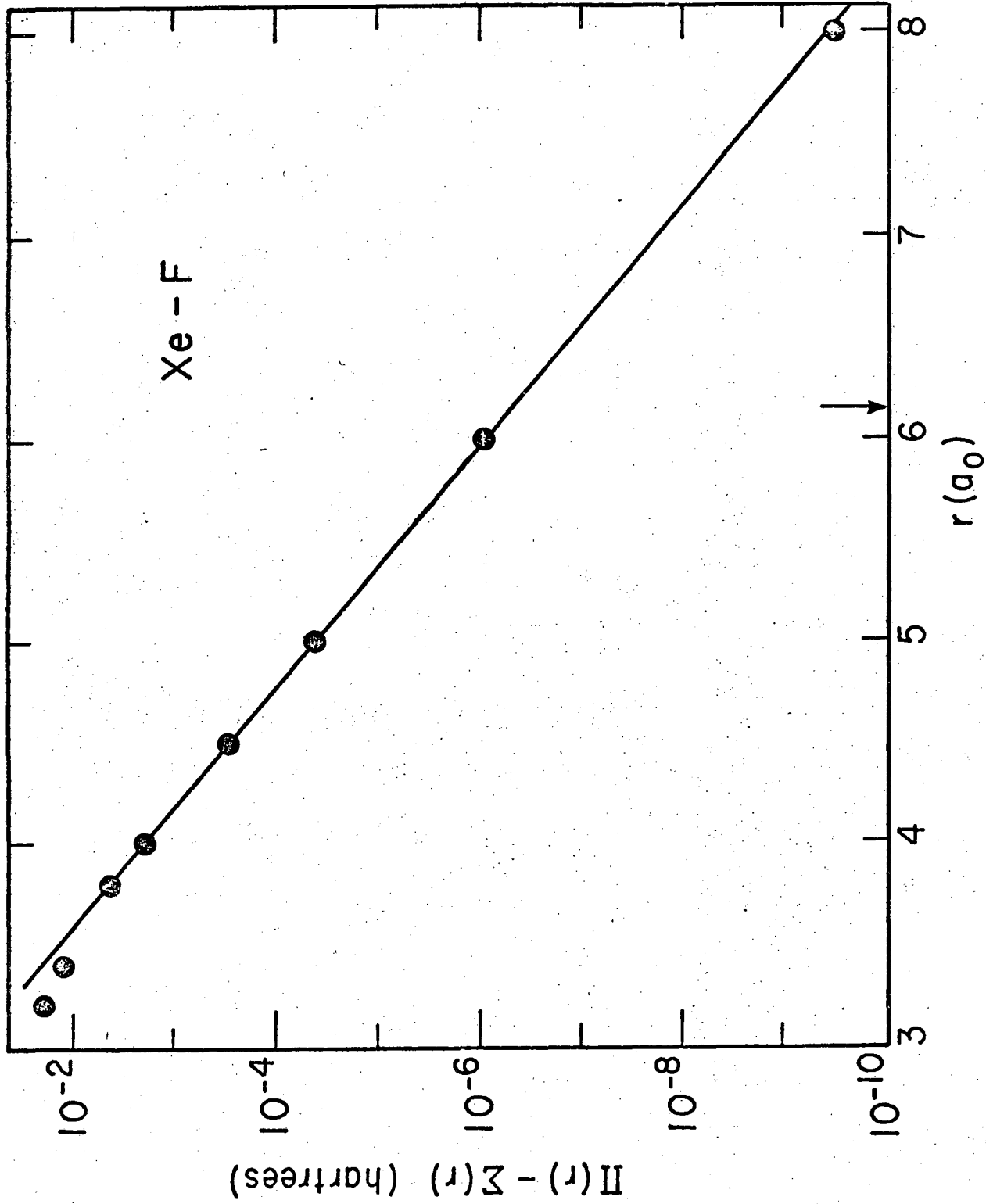
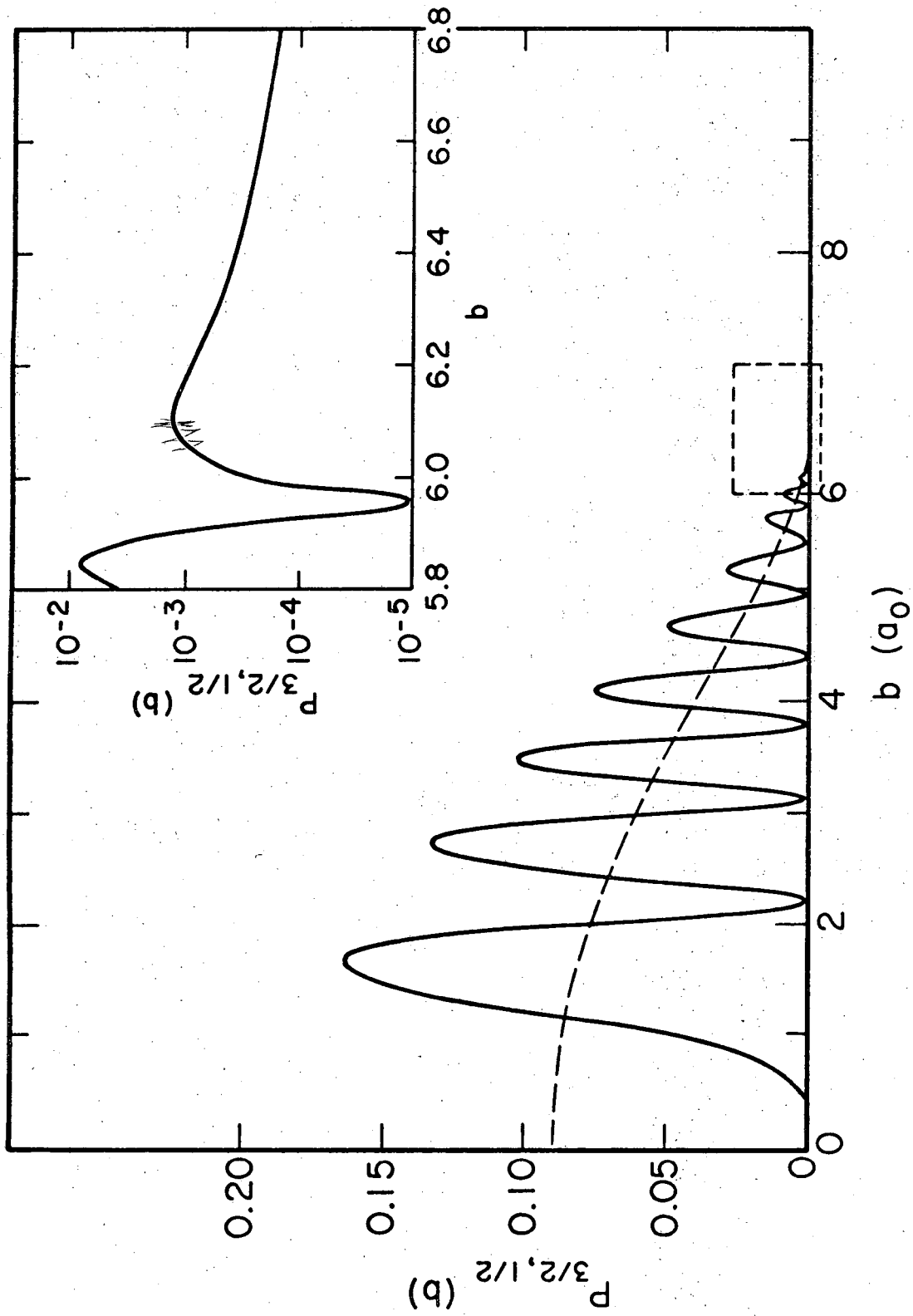


Fig. 1

XBL 741-5496



XBL 741-5418

Fig. 2

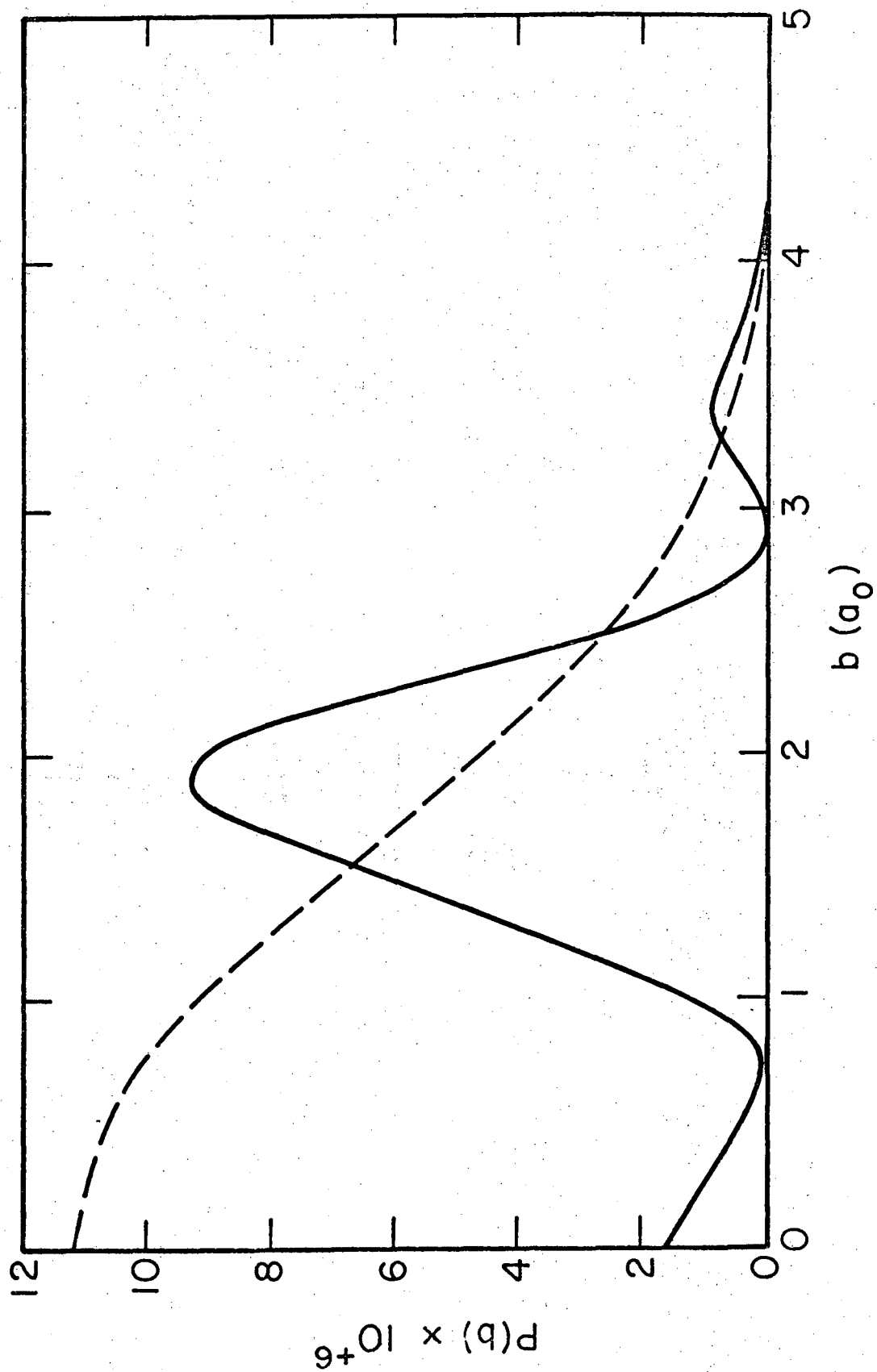
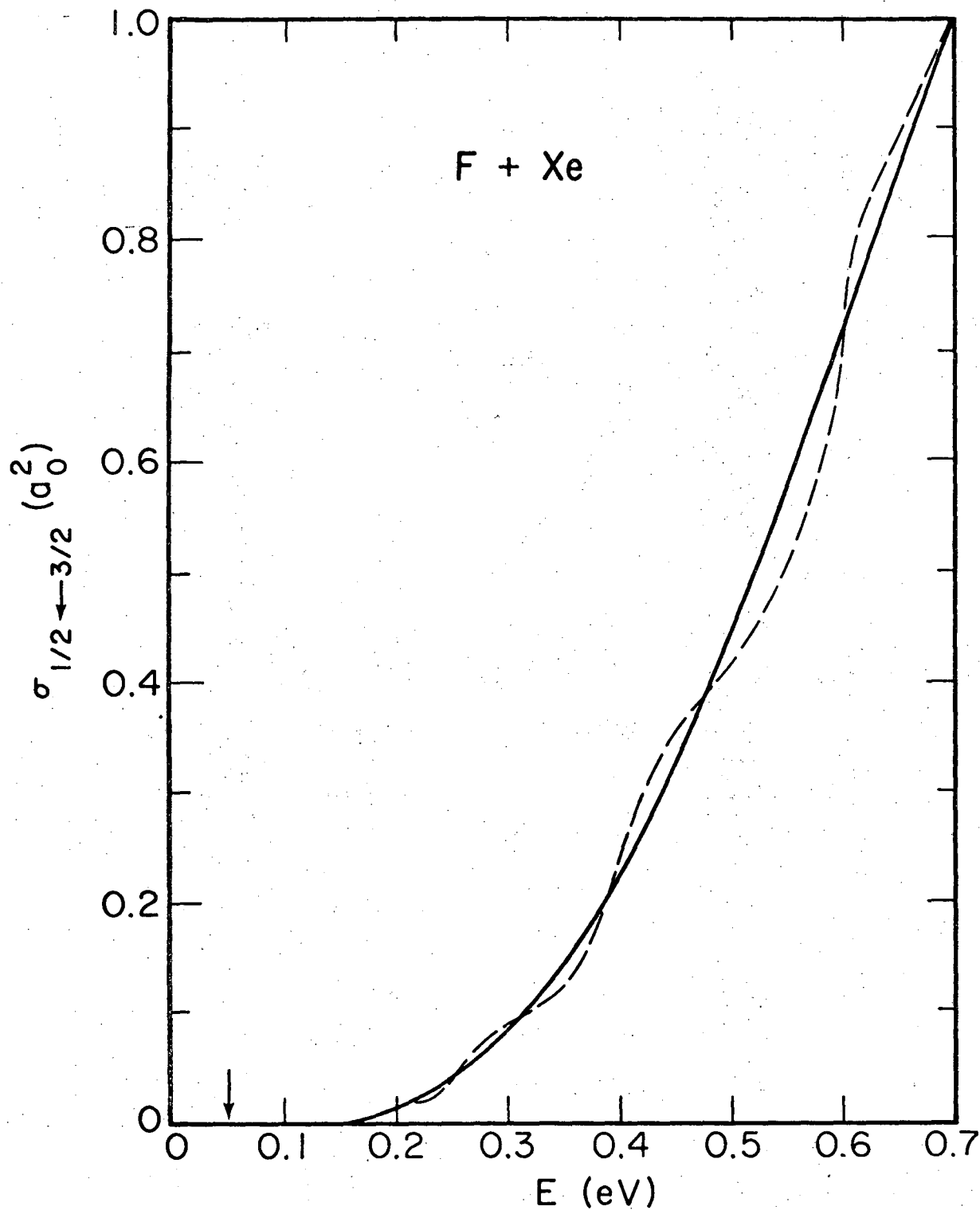
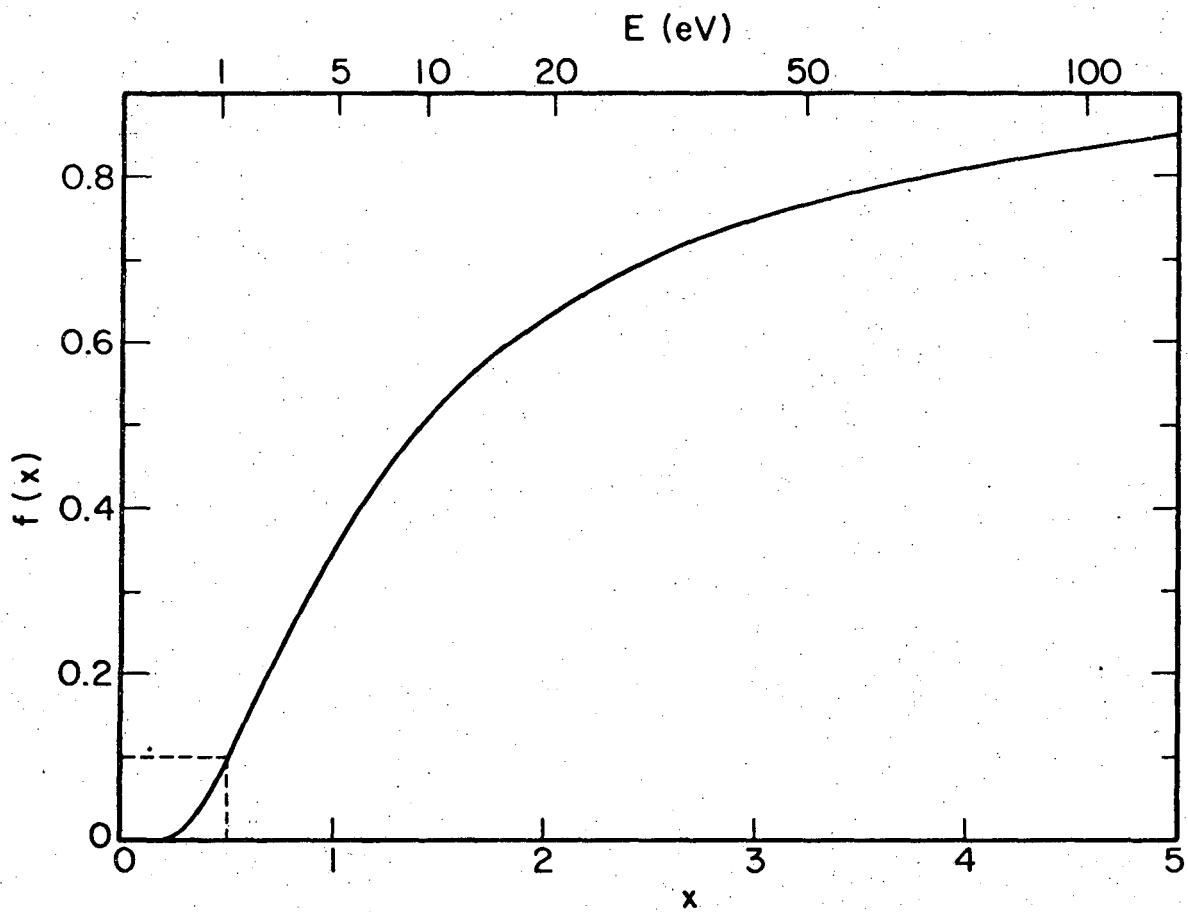


Fig. 3



XBL 741-5409

Fig. 4



XBL 741-5415

Fig. 5

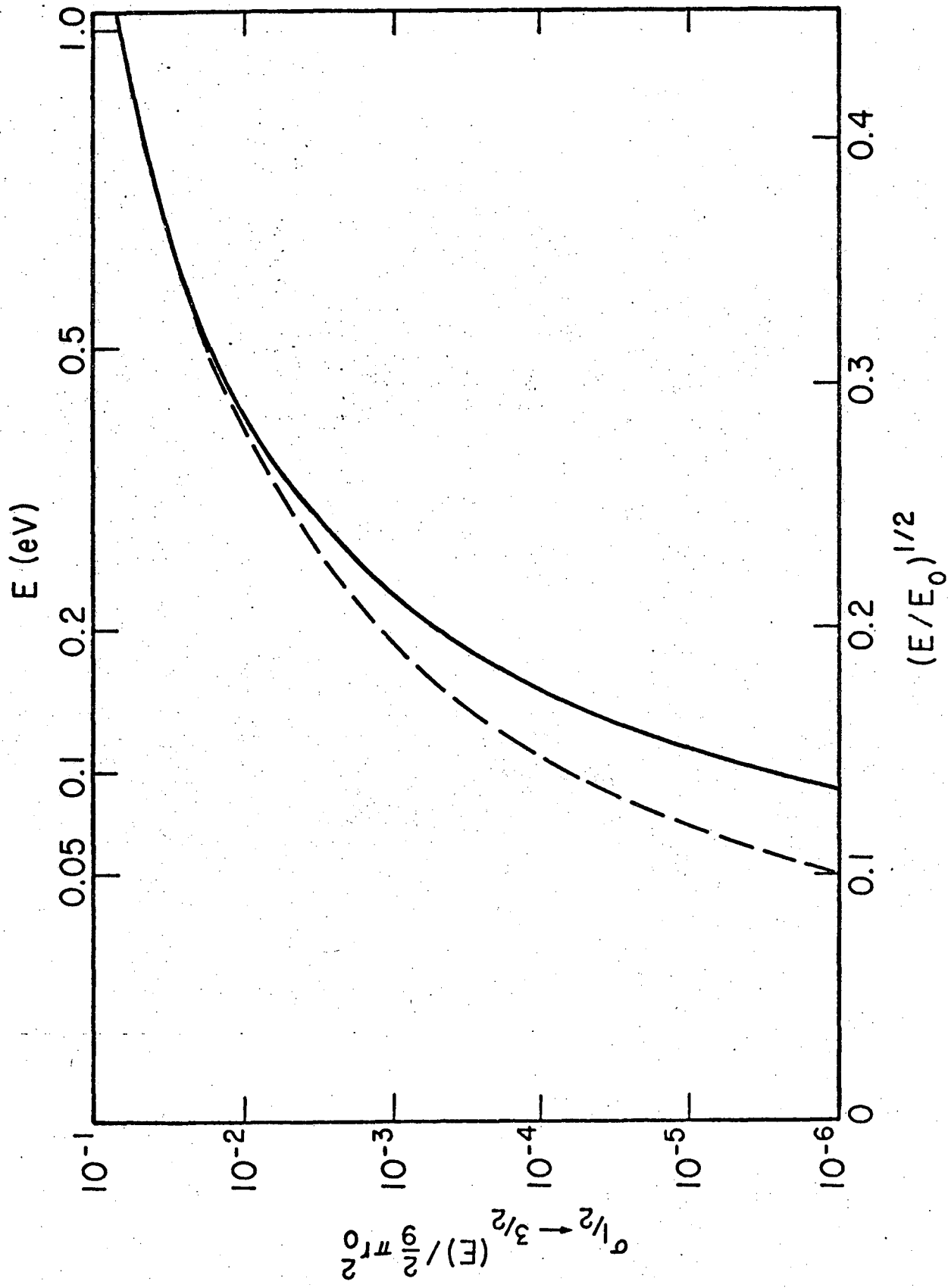
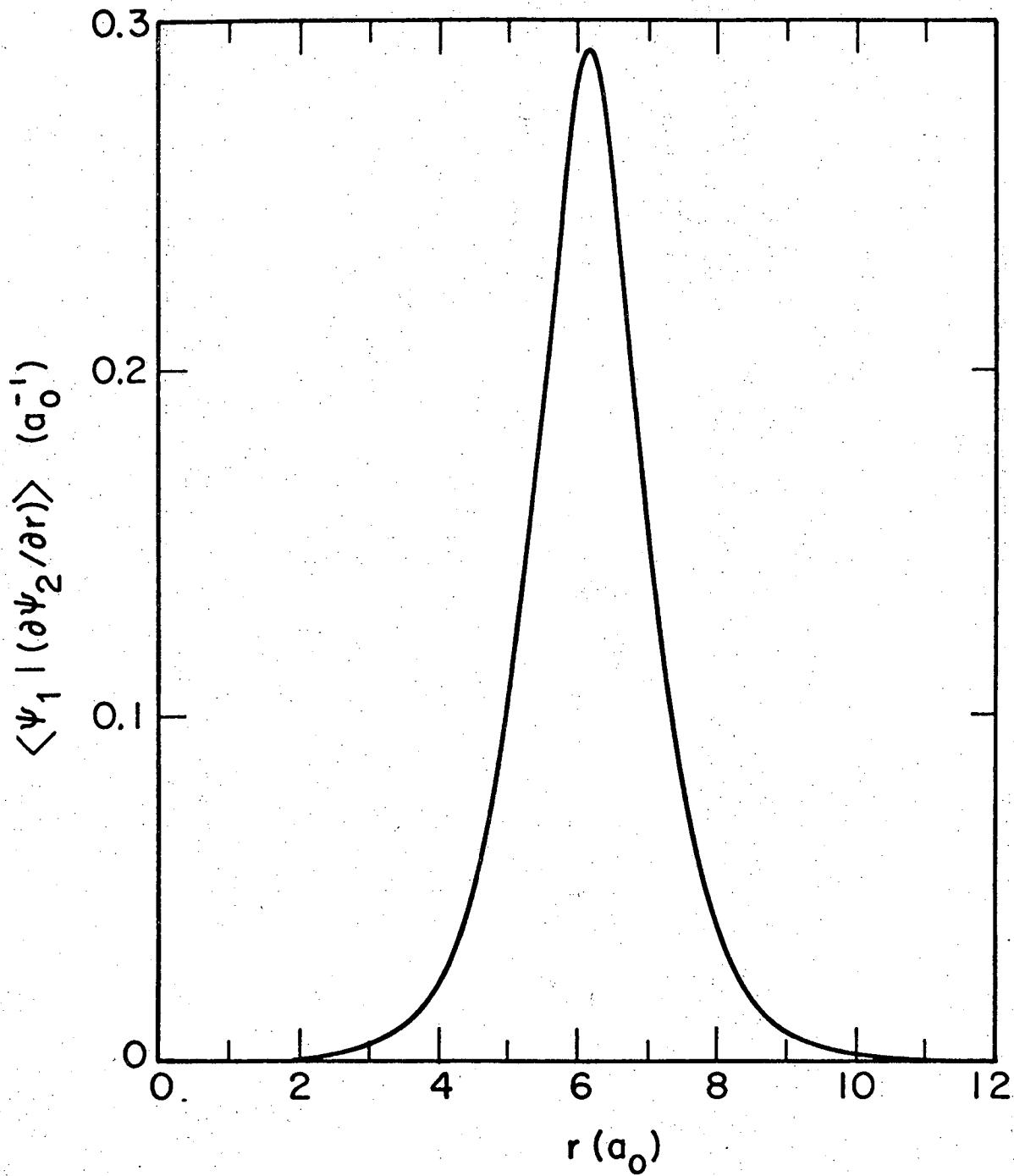


Fig. 6



XBL 741-5411

Fig. 7

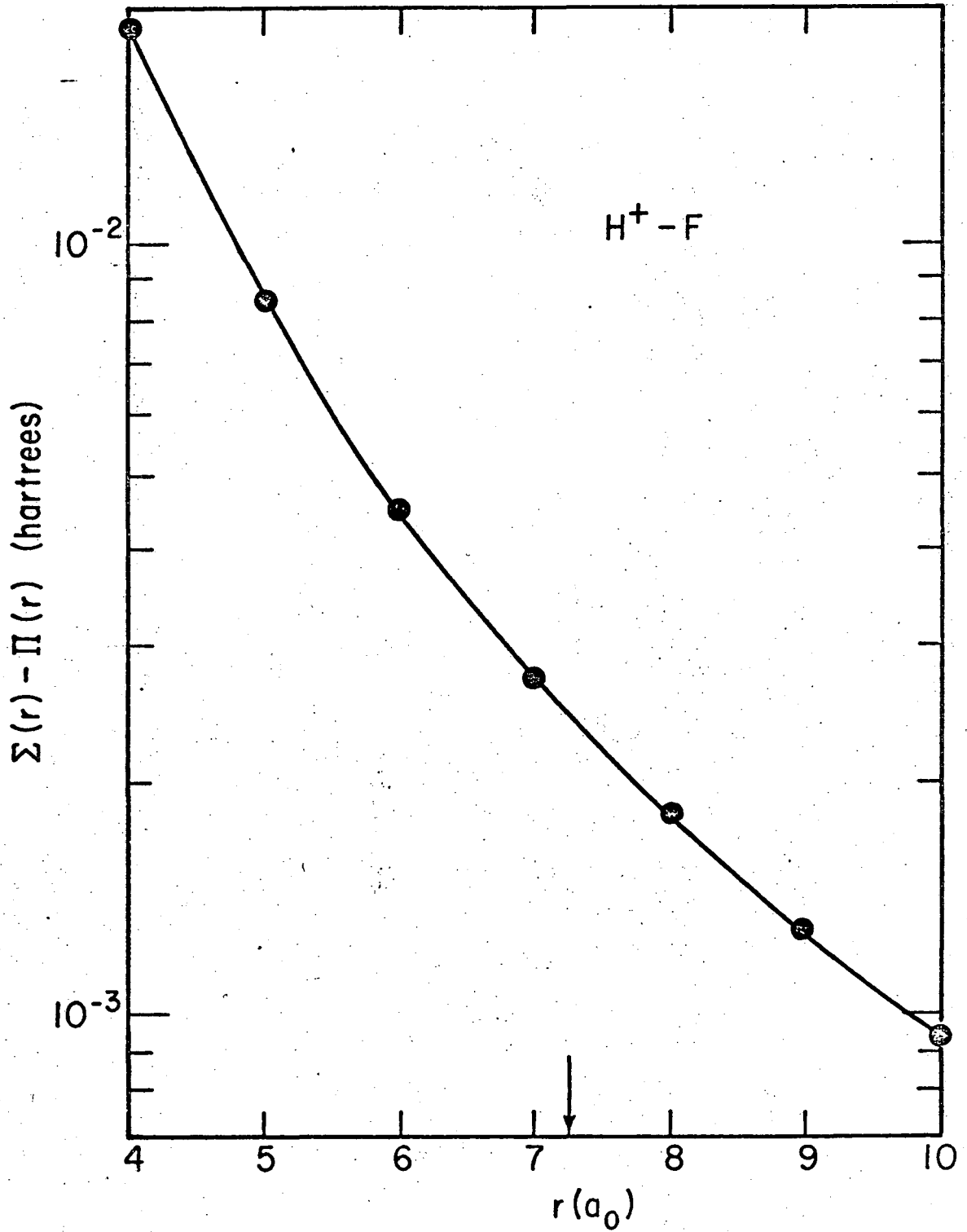


Fig. 8

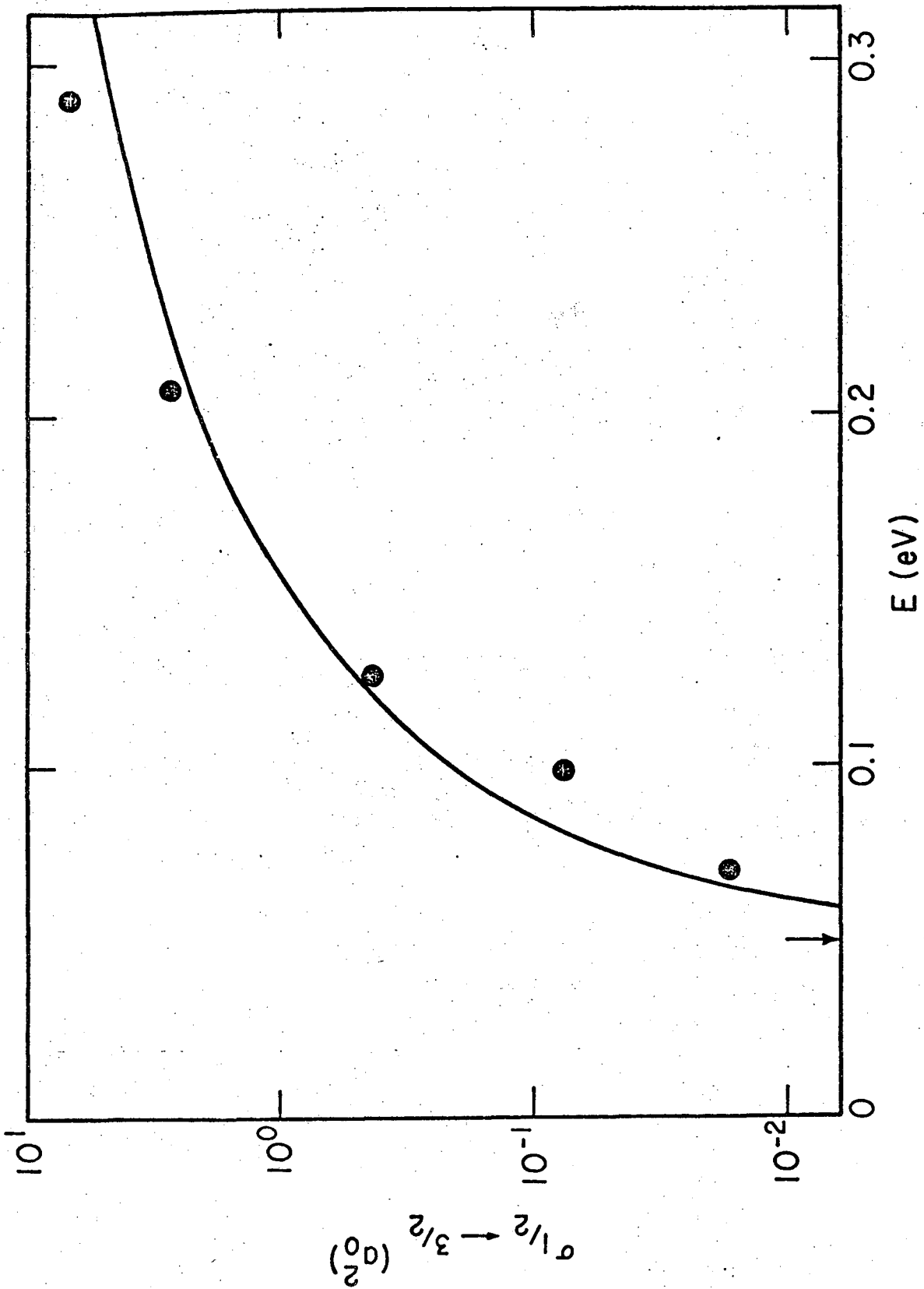


FIG. 9

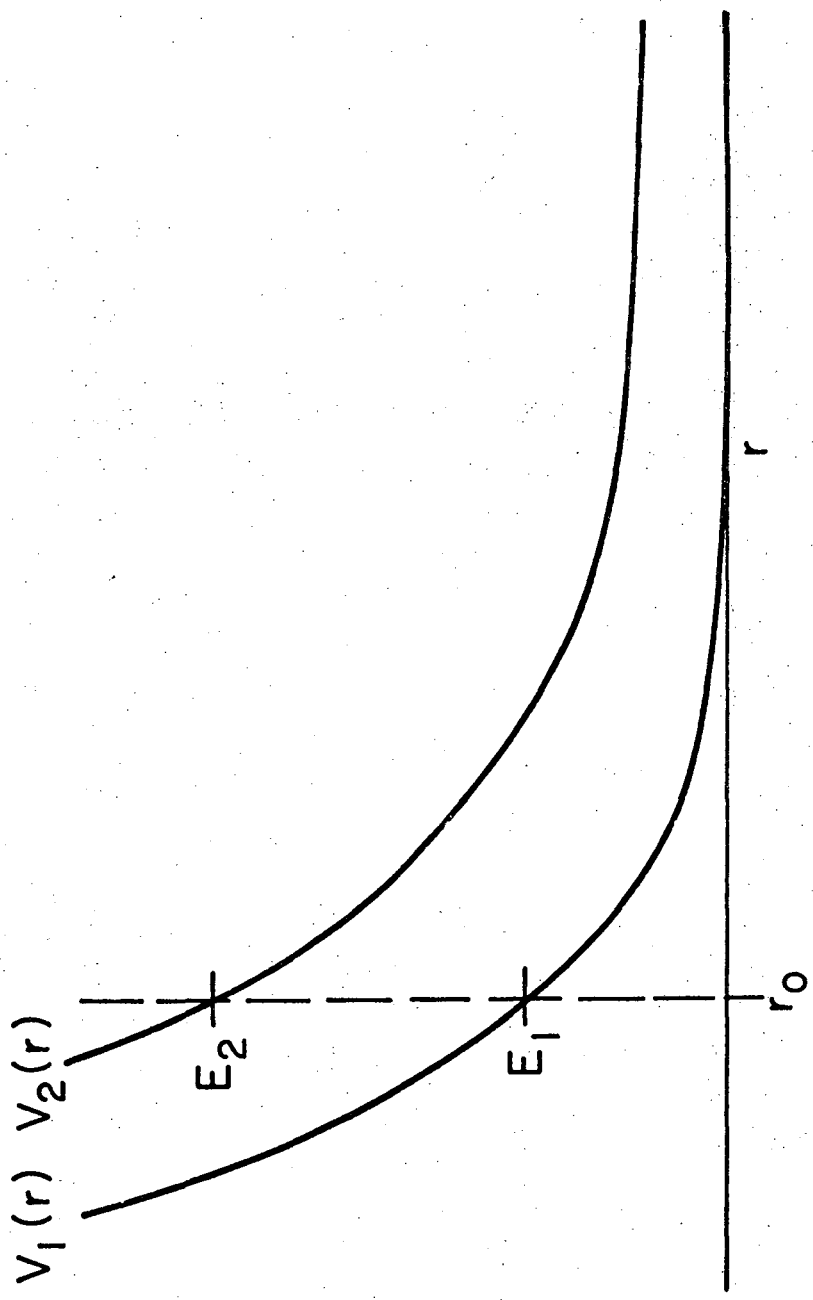


Fig. 10

LEGAL NOTICE

This report was prepared as an account of work sponsored by the United States Government. Neither the United States nor the United States Atomic Energy Commission, nor any of their employees, nor any of their contractors, subcontractors, or their employees, makes any warranty, express or implied, or assumes any legal liability or responsibility for the accuracy, completeness or usefulness of any information, apparatus, product or process disclosed, or represents that its use would not infringe privately owned rights.

TECHNICAL INFORMATION DIVISION
LAWRENCE BERKELEY LABORATORY
UNIVERSITY OF CALIFORNIA
BERKELEY, CALIFORNIA 94720